

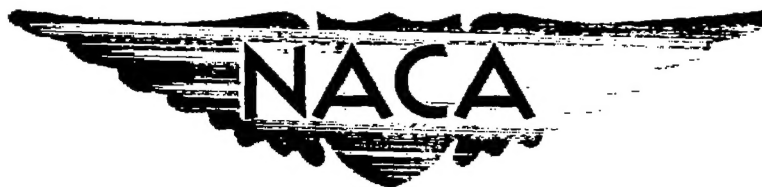
UNCLASSIFIED

CONFIDENTIAL

Copy

RM A54C04

NACA RM A54C04



# RESEARCH MEMORANDUM

EXPERIMENTAL INVESTIGATION OF THE AERODYNAMIC  
CHARACTERISTICS OF A BALLISTIC-TYPE MISSILE

By Stanford E. Neice

Ames Aeronautical Laboratory  
Moffett Field, Calif.

CLASSIFICATION CHANGED

To UNCLASSIFIED

By authority of NASA TPA 8 *Effective* Date 7-22-57  
*NB 9-14-57*

CLASSIFIED DOCUMENT

This material contains information affecting the National Defense of the United States within the meaning of the espionage laws, Title 18, U.S.C., Secs. 793 and 794; the transmission or revelation of which in any manner to an unauthorized person is prohibited by law.

**NATIONAL ADVISORY COMMITTEE  
FOR AERONAUTICS LIBRARY COPY**

WASHINGTON

APR 28 1954

April 23, 1954

LANGLEY AERONAUTICAL LABORATORY  
LIBRARY, NACA  
LANGLEY FIELD, VIRGINIA

CONFIDENTIAL

UNCLASSIFIED

1J  
NACA RM A54C04

3 1176 01434 7810

UNCLASSIFIED

## NATIONAL ADVISORY COMMITTEE FOR AERONAUTICS

RESEARCH MEMORANDUM

## EXPERIMENTAL INVESTIGATION OF THE AERODYNAMIC

## CHARACTERISTICS OF A BALLISTIC-TYPE MISSILE

By Stanford E. Neice

## SUMMARY

Lift, drag, and pitching-moment coefficients of a ballistic-type-missile configuration have been determined from tests in the Ames 10- by 14-inch supersonic wind tunnel at Mach numbers from 2.75 to 6.3 and at angles of attack from  $0^\circ$  to  $16^\circ$ . Pressure distributions and pressure-drag coefficients were also determined at  $0^\circ$  angle of attack.

The missile consisted of a cone-cylinder combination with a long slender spike added to the nose of the cone. As a consequence of the lift carry-over to the forward part of the cylindrical afterbody, the slopes of the lift and pitching-moment-coefficient curves at  $0^\circ$  angle of attack were found to be considerably larger than the predictions of Newtonian impact theory.

At Mach numbers up to 5.0, the pressure-drag coefficient of the missile was equal to that of a  $10^\circ$  cone even though there was an over-compression of the flow at the concave corner between the spike and main conical section. However, at Mach number 6.3, where the Reynolds number was very low, there was an appreciable increase in pressure drag. This effect, coupled with an increase in skin-friction coefficient, resulted in a marked increase in total drag coefficient at the highest test Mach number.

## INTRODUCTION

A test program was undertaken in the Ames 10- by 14-inch supersonic wind tunnel to determine the aerodynamic characteristics of a ballistic-type-missile configuration consisting of a cone-cylinder combination with a long slender spike added to the nose of the cone. In particular, lift, drag, and pitching moments were obtained at Mach numbers from 2.75 to 6.3 and at angles of attack from  $0^\circ$  to  $16^\circ$ .

  
UNCLASSIFIED

During the course of this investigation it was found that, at the highest test Mach numbers, the drag near  $0^\circ$  angle of attack was appreciably larger than would be expected. In order to study this matter, pressures acting on the model at zero incidence were obtained throughout the Mach number range.

The purpose of the present paper is to report the results of this investigation.

#### NOTATION

A	base area of model
$C_D$	drag coefficient, $\frac{\text{drag}}{q_0 A}$
$C_L$	lift coefficient, $\frac{\text{lift}}{q_0 A}$
$C_m$	pitching-moment coefficient about model base, $\frac{\text{pitching moment}}{q_0 A l}$
$C_p$	pressure coefficient, $\frac{p - p_0}{q_0}$
$l$	model length
M	Mach number
p	static pressure
q	dynamic pressure
$\alpha$	angle of attack

#### Subscripts

o	free-stream conditions
---	------------------------

#### APPARATUS

##### Wind Tunnel

Tests were conducted in the Ames 10- by 14-inch supersonic wind tunnel. A detailed description of the wind tunnel and auxiliary operating equipment may be found in reference 1.

## Models and Testing Equipment

Balance tests.- A model of a ballistic-type missile was used in this part of the investigation. The model was constructed of steel with a 0.0002-inch-thick chromium plate. The dimensions of the model are given in figure 1.

The aerodynamic forces and moments acting on the model were measured by a three-component strain-gage balance. Angles of attack up to  $5^{\circ}$  were obtained by rotating the balance assembly. Angles of attack greater than  $5^{\circ}$  were obtained by the use of bent-sting model supports. Forces acting on the model base were determined from base pressures measured with a U-tube manometer.

Pressure-distribution tests.- The pressure-distribution model was twice the size of the model used in the force and moment tests. The metal and plating requirements were identical. The cylindrical afterbody, which does not contribute to the pressure foredrag at  $0^{\circ}$  angle of attack, was shortened in order to enable the entire model to be positioned within a region of uniform flow in the test section. The dimensions of the pressure-distribution model and the location of the pressure orifices are given in figure 2.

At Mach numbers 2.75 and 3.0, pressures on the model surface were measured with a mercury U-tube manometer. The lower pressures encountered above Mach number 3.0 were measured by means of McCleod gages.

## TESTS AND PROCEDURE

### Balance Tests

Lift, drag, and pitching-moment coefficients were determined at angles of attack from  $0^{\circ}$  to about  $16^{\circ}$  and Mach numbers of 2.75, 4.2, and 6.3. At Mach number 3.0, tests were conducted at angles of attack up to  $10^{\circ}$ . At Mach number 5.0, tests were conducted only at  $0^{\circ}$  angle of attack. The variation of free-stream Reynolds number per foot with test Mach number is given in figure 3.

The measured forces and moments were corrected for the effects of balance buoyancy (pressure gradients existing within the balance housing) and for free-stream buoyancy (pressure gradients in the free stream). The forces on the model base, as determined from base-pressure readings, were subtracted from the measured forces acting on the entire model. All data, therefore, represent the effect of forces acting on the forward part of the model, exclusive of the base.

### Pressure-Distribution Tests

Pressures on the model surface were measured at  $0^\circ$  angle of attack and at test Mach numbers of 2.75, 3.0, 4.2, 5.0, and 6.3. The measured pressures were converted to the form of pressure coefficients and were integrated graphically to obtain pressure-drag coefficients.

### ACCURACY OF TEST RESULTS

In the region of the test section where the model was located, the variation in Mach number from the nominal value did not exceed  $\pm 0.02$  for nominal Mach numbers from 2.75 to 5.0 and  $\pm 0.04$  at Mach number 6.3. Corresponding variations in free-stream static pressure were sufficiently small so that free-stream buoyancy corrections were necessary only at Mach numbers 2.75 and 3.0.

Deviations in free-stream Reynolds number per foot for a given test Mach number did not exceed  $\pm 10,000$  from the values given in figure 3.

### Balance Tests

The estimated maximum errors in the angle-of-attack values were  $\pm 0.2^\circ$  and were due to uncertainties in the corrections for stream angle and the deflection of the model support system.

Accuracy of the computed force and moment coefficients was affected by the errors in measurements of the balance system as well as by uncertainties in the free-stream dynamic pressures, base pressures, and pressure gradients within the balance housing. At Mach number 6.3, the low free-stream dynamic pressure leads to reduced accuracy of these coefficients.

At low angles of attack, the maximum probable errors in lift and drag coefficients are  $\pm 0.008$  at Mach numbers from 2.75 to 5.0 and  $\pm 0.025$  at Mach number 6.3. At angles of attack above  $10^\circ$ , these errors increased to  $\pm 0.015$  for Mach numbers from 2.75 to 5.0 and  $\pm 0.040$  at Mach number 6.3. The corresponding errors in pitching-moment coefficients are  $\pm 0.020$  for Mach numbers from 2.75 to 5.0 and  $\pm 0.040$  at Mach number 6.3. These errors did not change appreciably throughout the range of angles of attack used in the tests.

## Pressure-Distribution Tests

The precision of the computed pressure coefficients was affected by inaccuracies in the pressure measurement, and uncertainties in the stream angle and the free-stream dynamic pressure. The resulting errors in the pressure coefficients were no greater than  $\pm 0.002$  throughout the entire Mach number range. In the determination of zero-lift pressure-drag coefficients, the additional inaccuracies involved in the graphical integration increased the error to a value no greater than  $\pm 0.004$ .

## RESULTS AND DISCUSSION

The variations of lift, drag, and pitching-moment coefficients with angle of attack, as determined from the balance tests, are presented in figures 4(a) through 4(d) for Mach numbers 2.75, 3.0, 4.2, and 6.3, respectively. Of particular interest with regard to the lift and pitching-moment coefficients is the slope of the curves at  $0^\circ$  angle of attack. The initial lift-curve slope remains almost constant at a value of 0.052 per degree throughout the range of test Mach numbers. The initial moment-curve slope is 0.031 per degree at Mach number 2.75 and decreases slightly to a value of 0.028 per degree at Mach number 6.3. Theoretical values, computed on the basis of Newtonian impact theory (ref. 2), for the initial slope of the lift and pitching-moment curves are 0.034 and 0.022, respectively. The low values predicted by the Newtonian theory result from the omission of the contribution of the lift carry-over to the cylindrical afterbody at small angles of attack. This effect is considered in reference 3, where it is indicated that theoretical values for the initial lift-curve slope of a  $10^\circ$  cone-cylinder<sup>1</sup> combination may be obtained which are comparable to the experimental values presented for the ballistic-type missile.

The values given in figure 4 for the drag coefficient at  $0^\circ$  angle of attack are seen to increase appreciably at Mach number 6.3. In order to study this rise in drag coefficient, additional tests were conducted to determine the pressure distributions and pressure-drag coefficients at  $0^\circ$  angle of attack throughout the Mach number range.

The zero-lift pressure coefficients along the forward part of the test model are given in figures 5(a) through 5(e) for Mach numbers 2.75, 3.0, 4.2, 5.0, and 6.3, respectively. Theoretical values of the pressure coefficient over the  $5^\circ$  cone forming the nose of the spike were determined from reference 4. For the cylindrical portions of the body, theoretical pressure coefficients were obtained from reference 5. Theoretical solutions are not available for the  $5^\circ$  conical section, which forms the

---

<sup>1</sup>The angular designation for cones used throughout this report refers to the semivertex angle.

rearward part of the spike, or for the large  $10^\circ$  conical section. The values given in reference 4 for a  $10^\circ$  cone are, however, presented in figure 5 for the  $10^\circ$  conical section inasmuch as they represent a value toward which the experimental data appear to converge.

An important feature to be observed in figure 5 is the pressure distribution over the forward part of the  $10^\circ$  conical section. The pressures are considerably higher, at all Mach numbers, than those predicted for conical flow in reference 4. Downstream of the concave corner, the values of pressure coefficient converge to the conical flow values given by reference 4. This over-compression at the corner is a two-dimensional flow phenomenon similar to the over-expansion which occurs at the convex corner between a cone and a cylinder, this latter phenomenon being the basis of the computations given in reference 5, as well as of the theoretical discussion found in reference 6.<sup>2</sup>

Over the  $5^\circ$  conical section downstream of the nose spike, pressures appear to be influenced by the boundary layer. The influence of the boundary layer becomes more pronounced in this region at Mach numbers 5.0 and 6.3 where the lowest values of Reynolds number are encountered. At Mach number 6.3, in particular, it appears that the excess thickening of the boundary layer caused by the concave corner may have extended almost to the nose of the spike.

A boundary-layer effect is also noticed in the flow about the convex corner between the  $10^\circ$  conical section and the cylindrical afterbody. The region of pressure reduction behind this corner is considerably widened at Mach numbers 5.0 and 6.3.

Zero-lift pressure-drag coefficients, obtained by graphical integration of the pressure coefficients, are presented in figure 6. At Mach numbers up to 5.0, there is close agreement between the experimental pressure-drag coefficients for the test model and the theoretical values for a  $10^\circ$  cone (ref. 4) even though there is over-compression at the concave corner at the start of the  $10^\circ$  conical section of the test model. At Mach number 6.3 there is an appreciable increase in pressure drag which may be due, in part, to this two-dimensional-type flow phenomenon. At this Mach number, however, thickening, if not separation, of the boundary layer appears to increase the effective cone angle and hence the pressure drag of the conical section.

The high pressure-drag coefficient at Mach number 6.3, along with the anticipated increase in skin friction at the lower test Reynolds number (fig. 3), suggest a possible explanation for the high total drag

---

<sup>2</sup>Although reference 6 deals primarily with expanding flow about bodies of revolution, it is pointed out in that paper that a similar phenomenon can be expected on bodies with increasing slope downstream of the nose.

---



coefficients obtained in the balance tests. From consideration of the Reynolds numbers involved, it seems evident that, at all test Mach numbers, a laminar boundary layer existed over the surface of the body forward of the cylindrical afterbody. Schlieren observations tended to corroborate this contention and further indicated that the boundary layer over the cylindrical afterbody was turbulent at Mach numbers 2.75 to 4.2 and laminar at Mach numbers 5.0 and 6.3.

Calculations of the skin-friction drag coefficients were simplified by replacing everything ahead of the cylindrical afterbody with a  $10^\circ$  cone. Laminar skin friction over the assumed nose cone was calculated from references 7 and 8. The skin-friction drag coefficients for the cylindrical afterbody were computed for both laminar and turbulent boundary layers from references 8 and 9, respectively. The resultant skin-friction drag coefficients, computed on the basis of laminar flow on the nose cone and either turbulent or laminar flow on the cylindrical afterbody, were added to the experimental pressure-drag coefficients to obtain the total estimated drag coefficients. The variations with Mach number of the measured and estimated total zero-lift drag coefficients are presented in figure 6. At Mach numbers 2.75, 3.0, and 4.2, the results of the balance tests are seen to agree with the calculated values corresponding to a turbulent boundary layer over the cylindrical afterbody. At Mach numbers 5.0 and 6.3 the data agree with values calculated for a laminar boundary layer over the cylinder. Evidently, then, the increase in total drag coefficient between Mach numbers 5.0 and 6.3 can be attributed to the increase in pressure coefficients over the forward portion of the model, in addition to the increase in skin-friction drag of the cylindrical afterbody resulting from the reduction in Reynolds numbers.

### CONCLUSIONS

Lift, drag, and pitching-moment coefficients for a ballistic-type missile have been determined experimentally at Mach numbers from 2.75 to 6.3 and angles of attack from  $0^\circ$  to  $16^\circ$ . The pressure distributions and the pressure-drag coefficients at  $0^\circ$  angle of attack have been determined throughout the same range of Mach numbers. From the results of these tests, the following conclusions are drawn:

1. The slopes of the lift and pitching-moment-coefficient curves at  $0^\circ$  angle of attack are considerably greater than the values predicted by the Newtonian impact theory. The higher experimental values are, primarily, a consequence of the lift carry-over to the cylindrical afterbody. This lift carry-over phenomenon is not accounted for in the impact theory.

2. At  $0^\circ$  angle of attack, two-dimensional-type flow exists at the concave corner between the nose spike and the  $10^\circ$  conical section. As a result of this flow phenomenon, higher pressures than those predicted by



conical flow considerations were found to occur over the forward part of the  $10^\circ$  conical section. However, the pressure drag was equal to that of a  $10^\circ$  cone at Mach numbers up to 5.0. At Mach number 6.3, however, there is an appreciable increase in pressure drag. This effect, coupled with an increase in skin-friction coefficient, resulted in a marked increase in zero-lift drag coefficient at the highest test Mach number.

Ames Aeronautical Laboratory  
National Advisory Committee for Aeronautics  
Moffett Field, Calif., March 4, 1954

#### REFERENCES

1. Eggers, A. J., Jr., and Nothwang, George J.: The Ames 10- by 14-Inch Supersonic Wind Tunnel. NACA TN 3095, 1953.
2. Grimmering, G., Williams, E. P., and Young, G. B. W.: Lift on Inclined Bodies of Revolution in Hypersonic Flow. Jour. Aero. Sci., vol. 17, no. 11, Nov. 1950, pp. 675-690.
3. Van Dyke, Milton D.: First- and Second-Order Theory of Supersonic Flow Past Bodies of Revolution. Jour. Aero. Sci., vol. 18, no. 3, Mar. 1951, pp. 161-178.
4. Mass. Inst. of Tech., Dept. of Elect. Engr., Center of Analysis. Tables of Supersonic Flow Around Cones, by the Staff of the Computing Section, Center of Analysis, under the direction of Zdenek Kopal, Tech. Rept. No. 1. Cambridge, 1947.
5. Clippinger, R. F., Giese, J. H., and Carter, W. C.: Tables of Supersonic Flows About Cone-Cylinders. Part I - Surface Data. Aberdeen Proving Ground, Aberdeen, Md., BRL Rep. 729, 1950.
6. Eggers, A. J., Jr., and Savin, Raymond C.: Approximate Methods for Calculating the Flow About Nonlifting Bodies of Revolution at High Supersonic Airspeeds. NACA TN 2579, 1951.
7. Hantzsche, W., and Wendt, H. (Ronald Kay, trans., M. W. Rubesin, ed.): The Laminar Boundary Layer of a Circular Cone in Supersonic Flow at Zero Angle of Attack. Univ. of Calif., Berkeley, Engr. Res. Proj., 1947.
8. Van Driest, E. R.: Investigation of Laminar Boundary Layer in Compressible Fluids Using the Crocco Method. NACA TN 2597, 1952.
9. Van Driest, E. R.: Turbulent Boundary Layer in Compressible Fluids. Jour. Aero. Sci., vol. 18, no. 3, Mar. 1951, pp. 145-160.

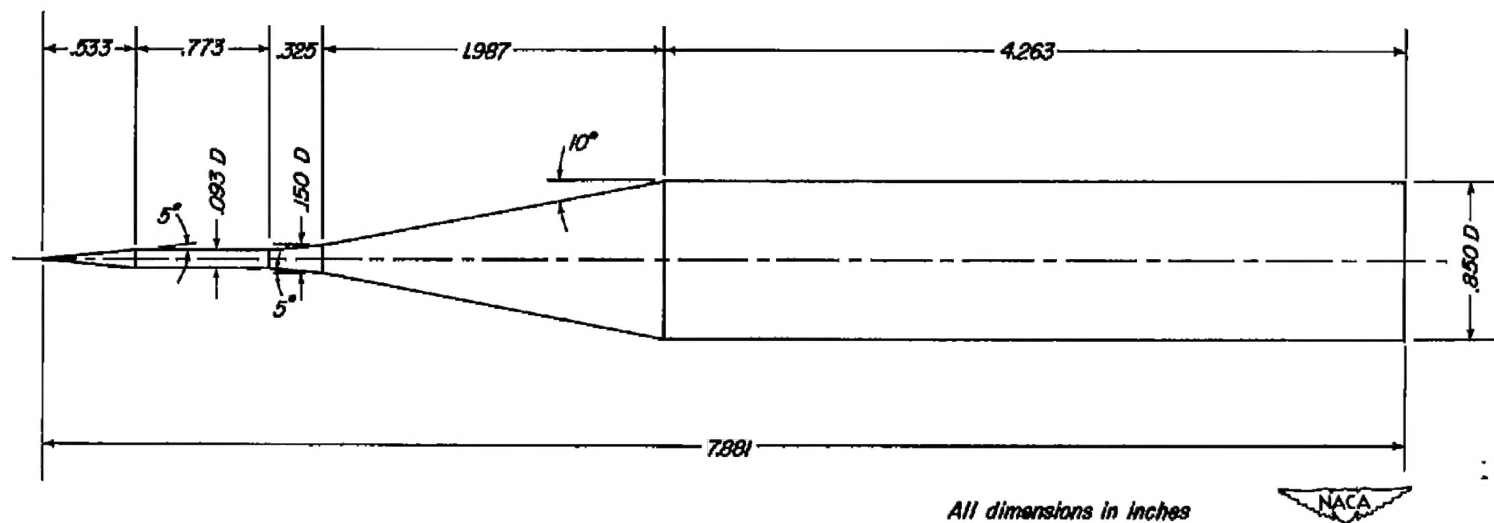


Figure 1.— Dimensions of balance test model of ballistic missile.

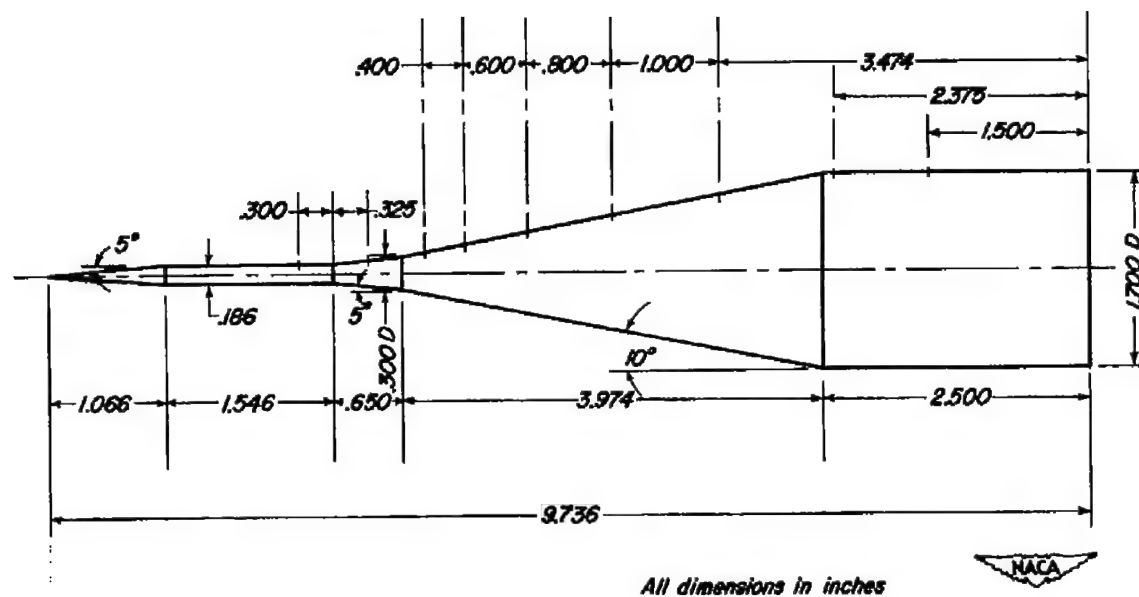


Figure 2.- Dimensions of pressure-distribution test model of ballistic missile showing location of pressure orifices.

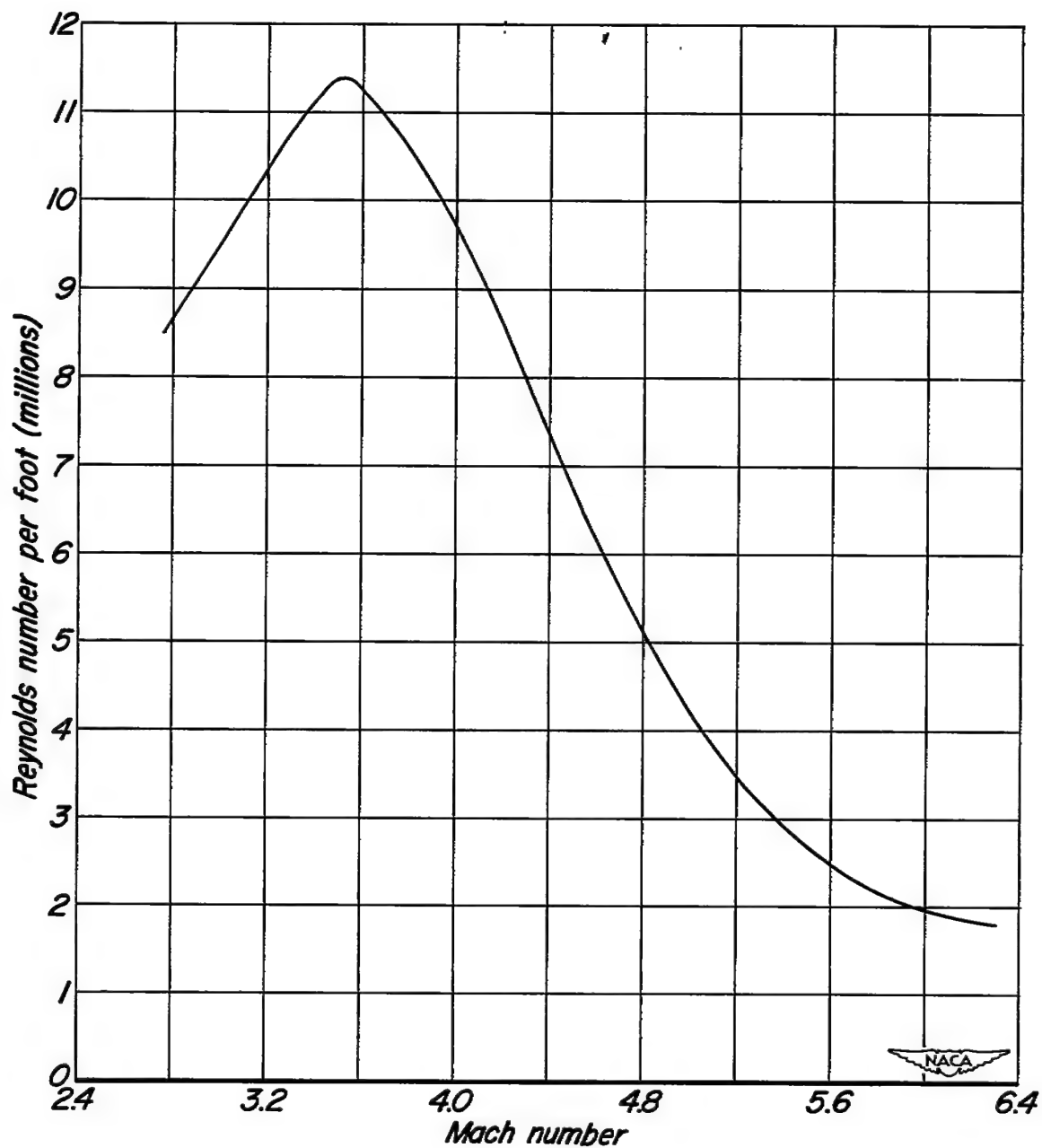


Figure 3.— Variation of Reynolds number with Mach number in the Ames 10- by 14-inch supersonic wind tunnel.

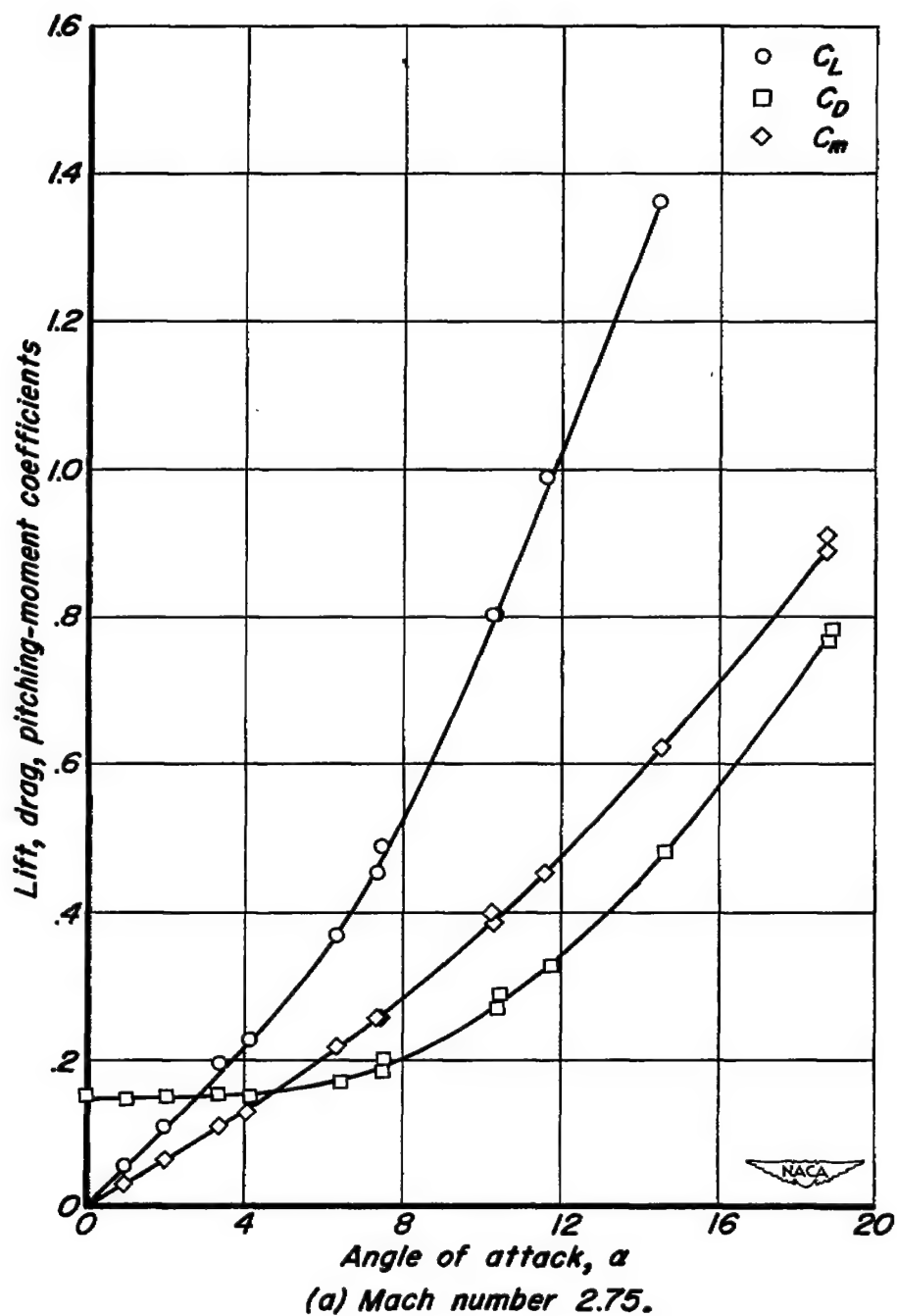


Figure 4.— Variation of lift, drag, and pitching-moment coefficients with angle of attack for ballistic missile.

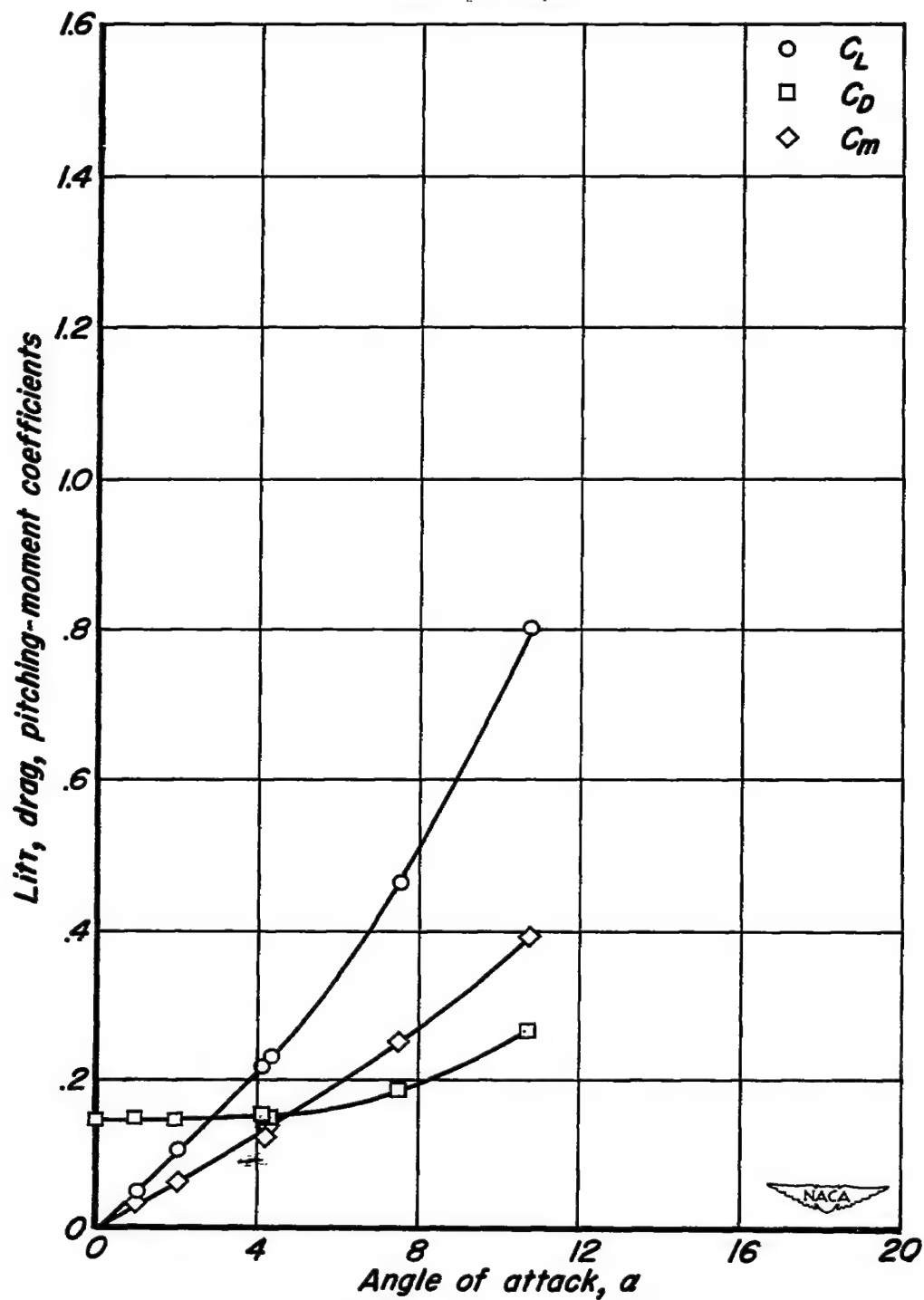
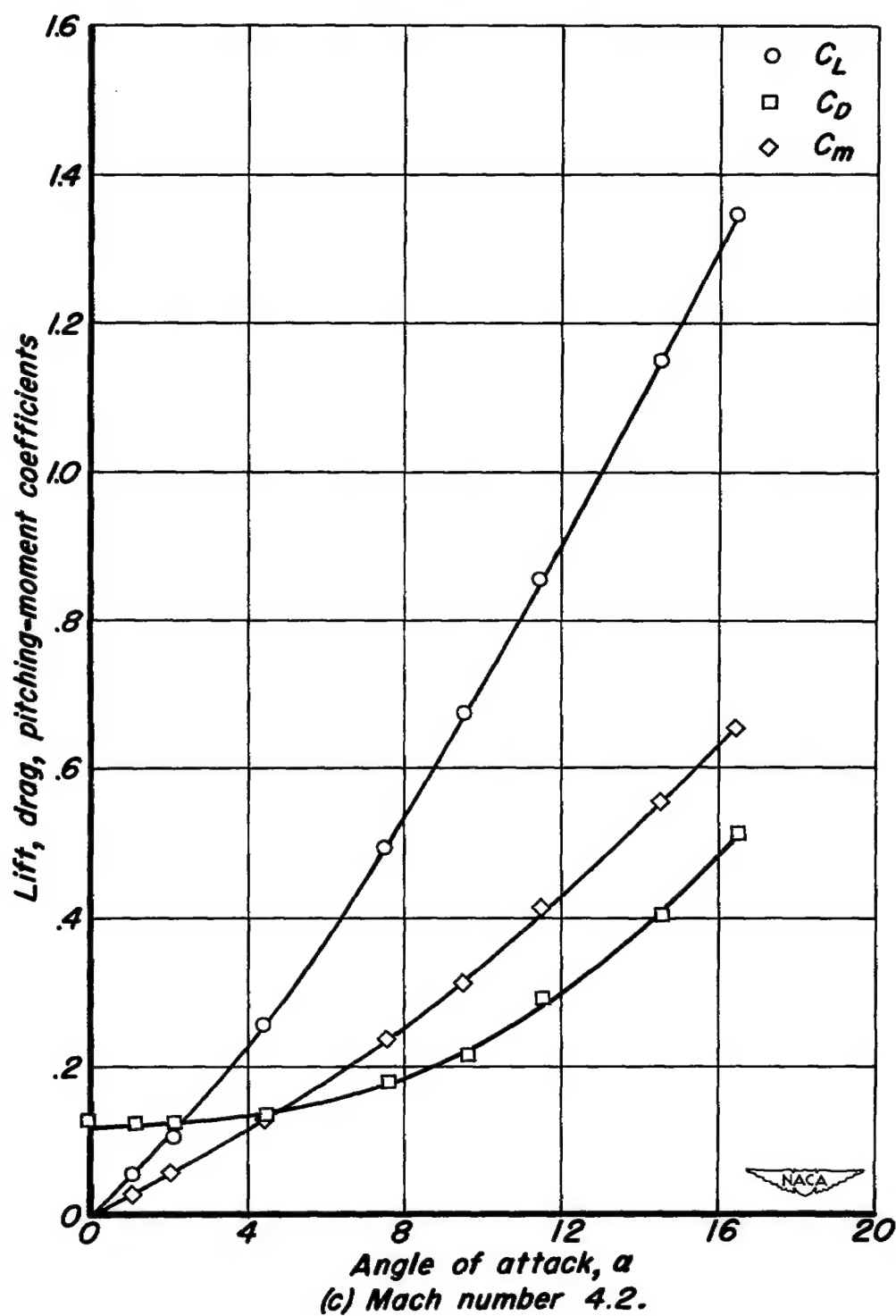
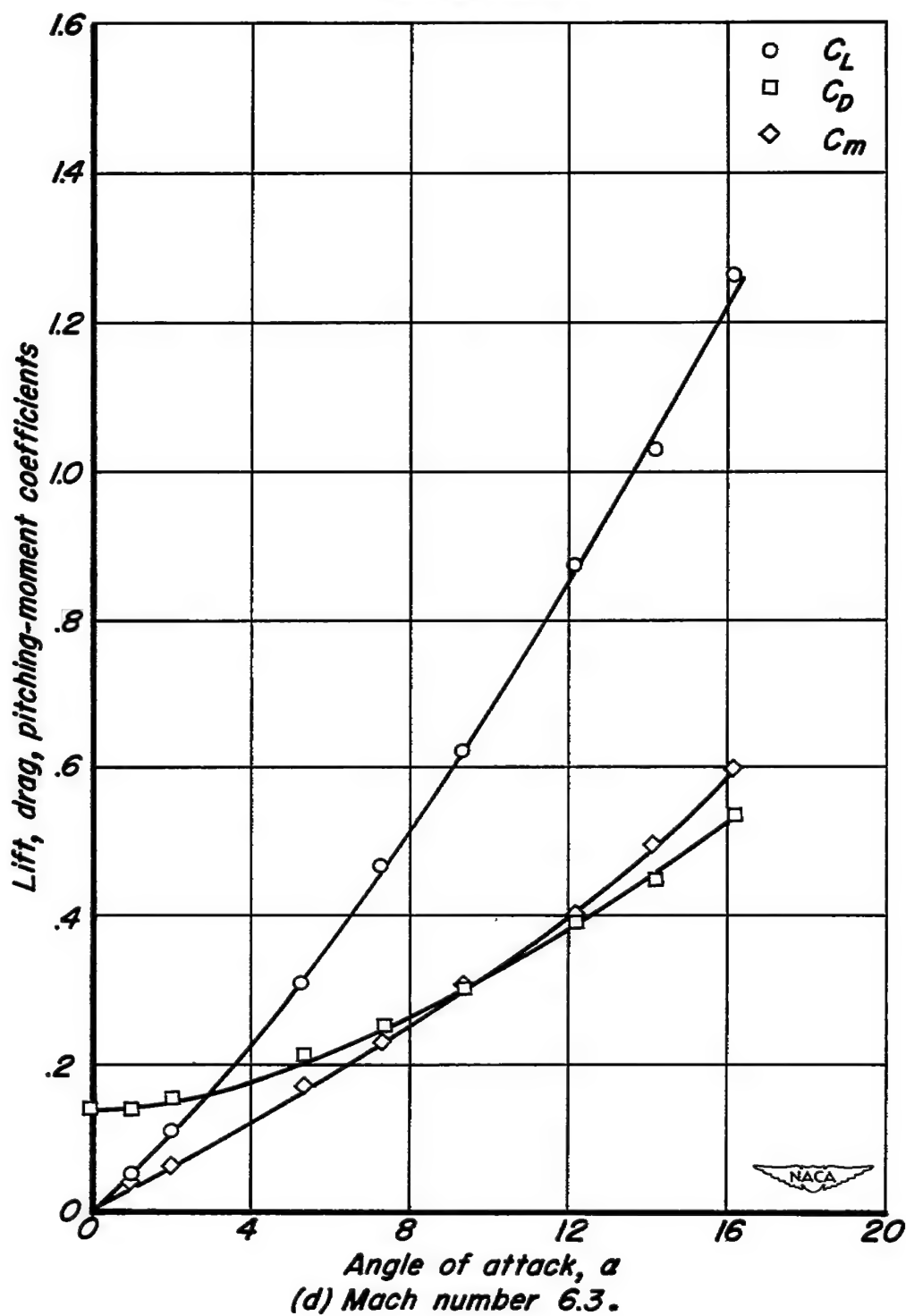
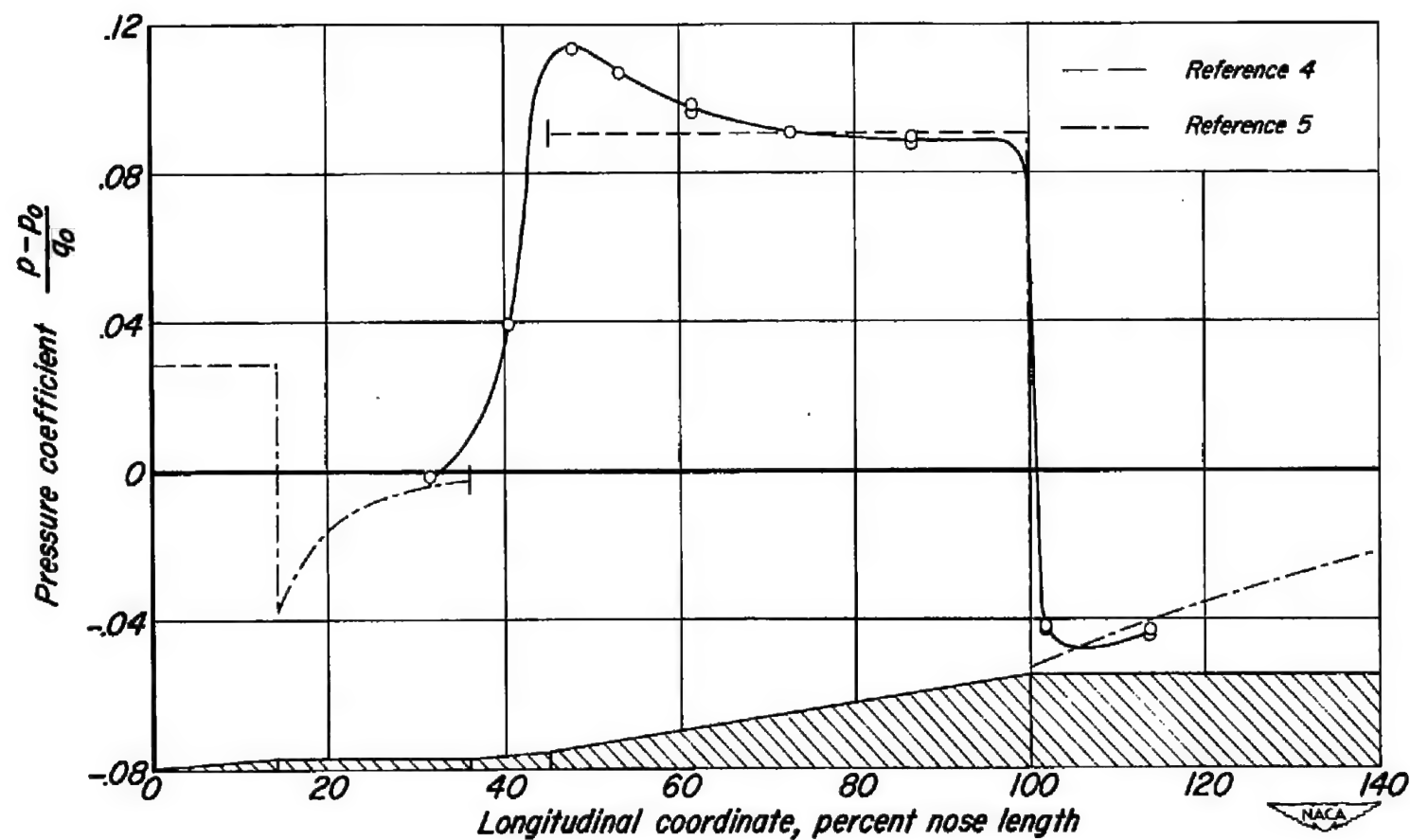


Figure 4.- Continued.



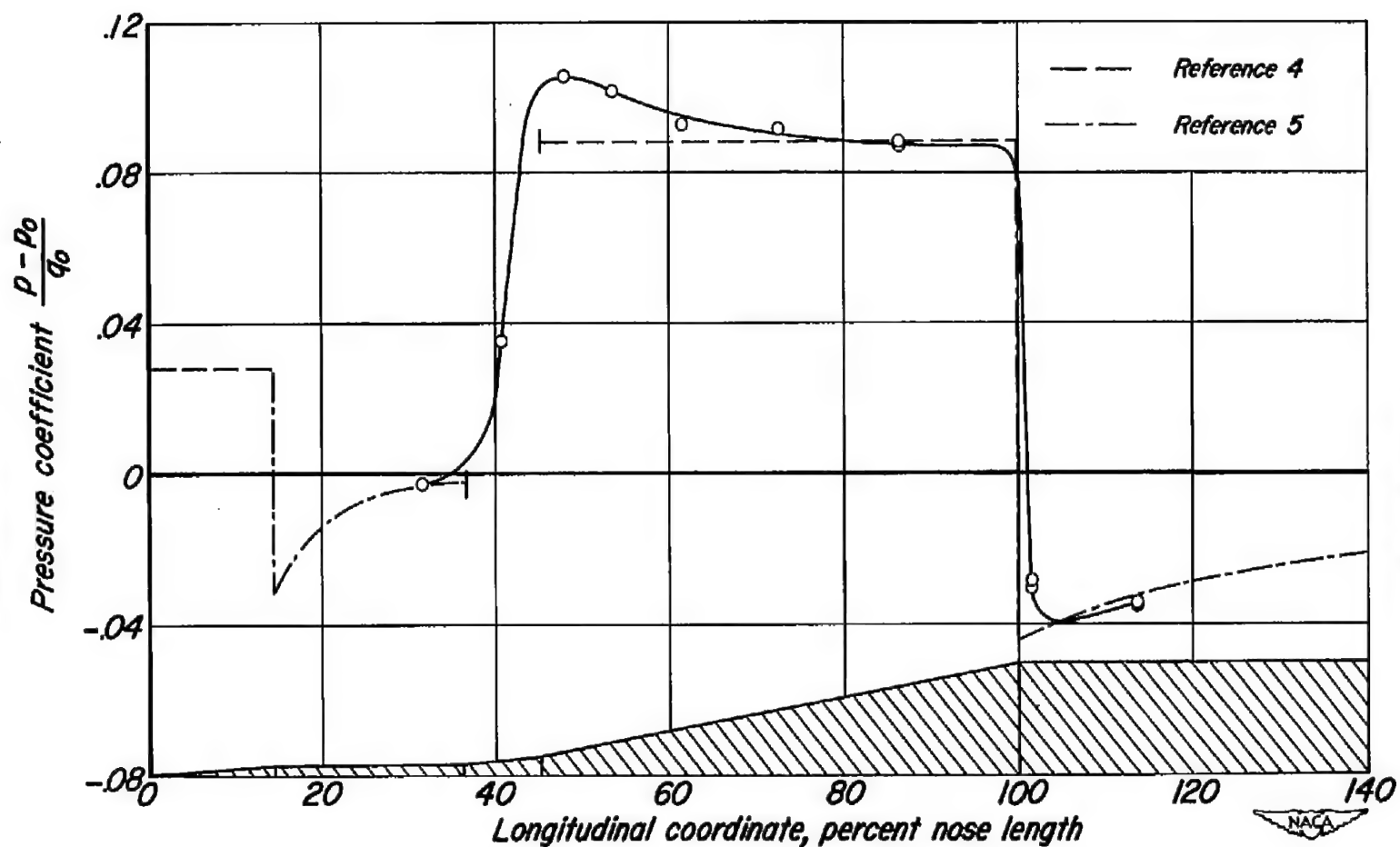






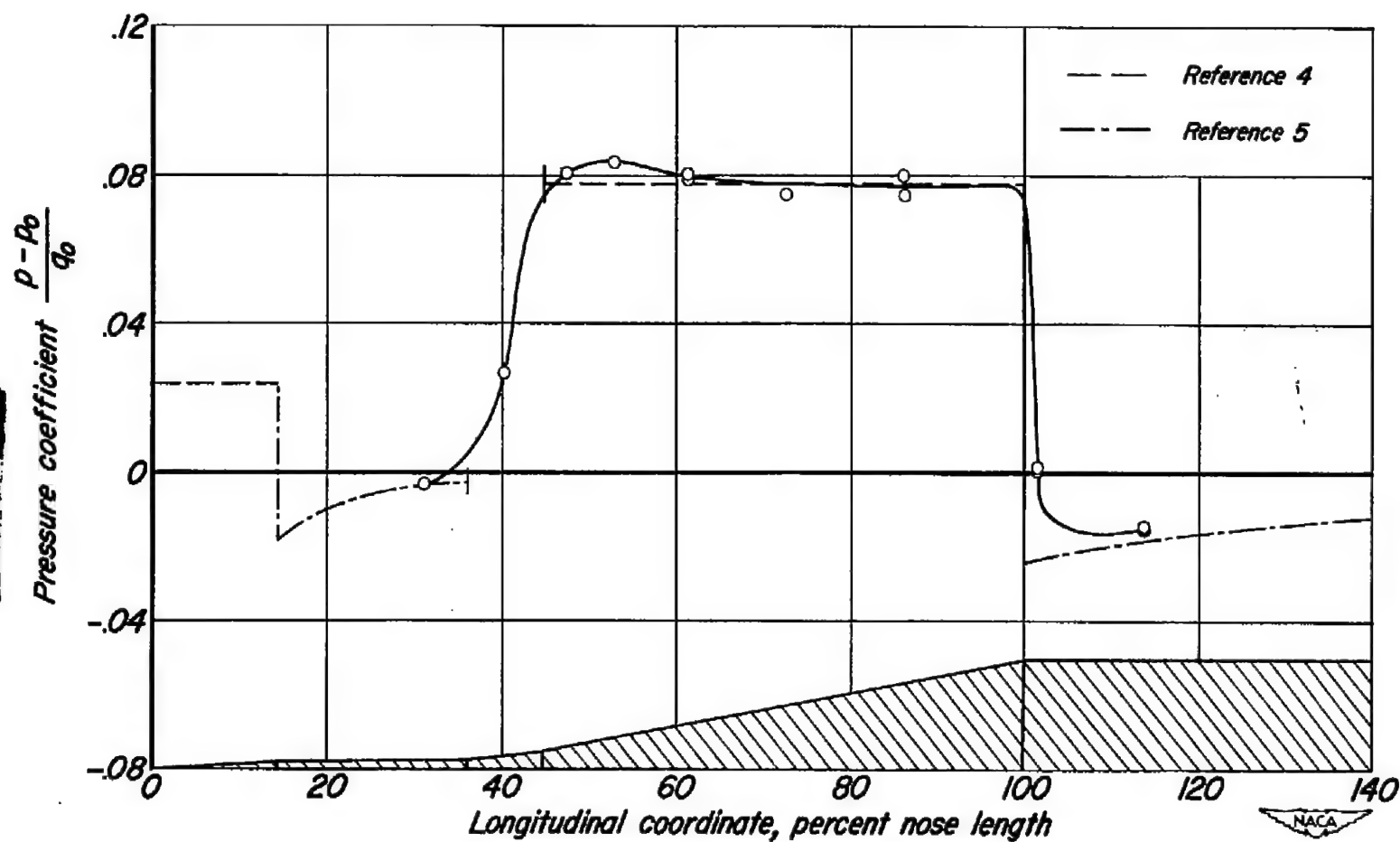
(a)  $M_0 = 2.75$

Figure 5.— Variation of zero-lift pressure coefficient along ballistic missile for given Mach numbers.



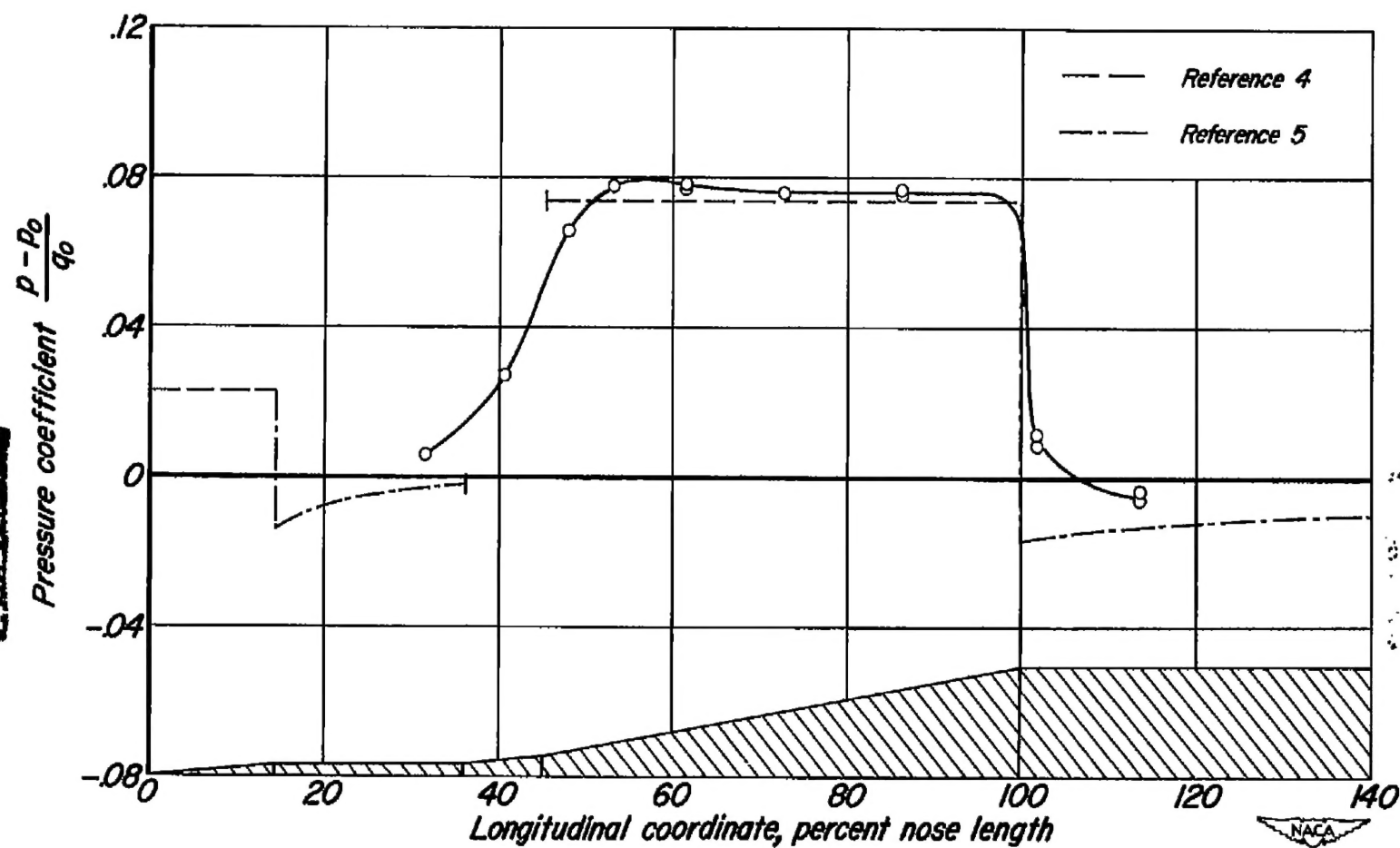
(b)  $M_0 = 3.0$

Figure 5.- Continued.



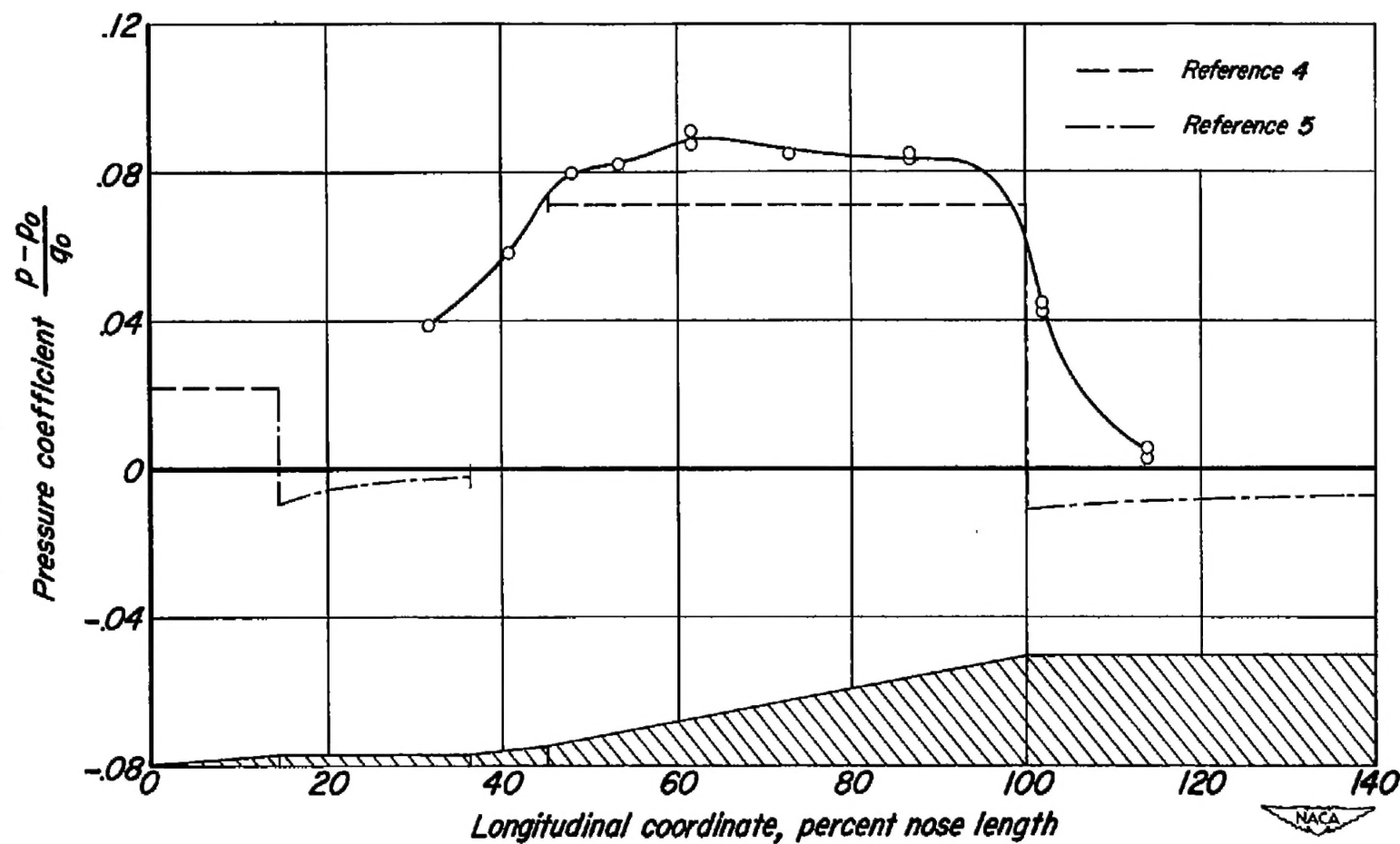
(c)  $M_0 = 4.2$

Figure 5.- Continued.



(d)  $M_0 = 5.0$

Figure 5.- Continued.



(e)  $M_0 = 6.3$

Figure 5.- Concluded.

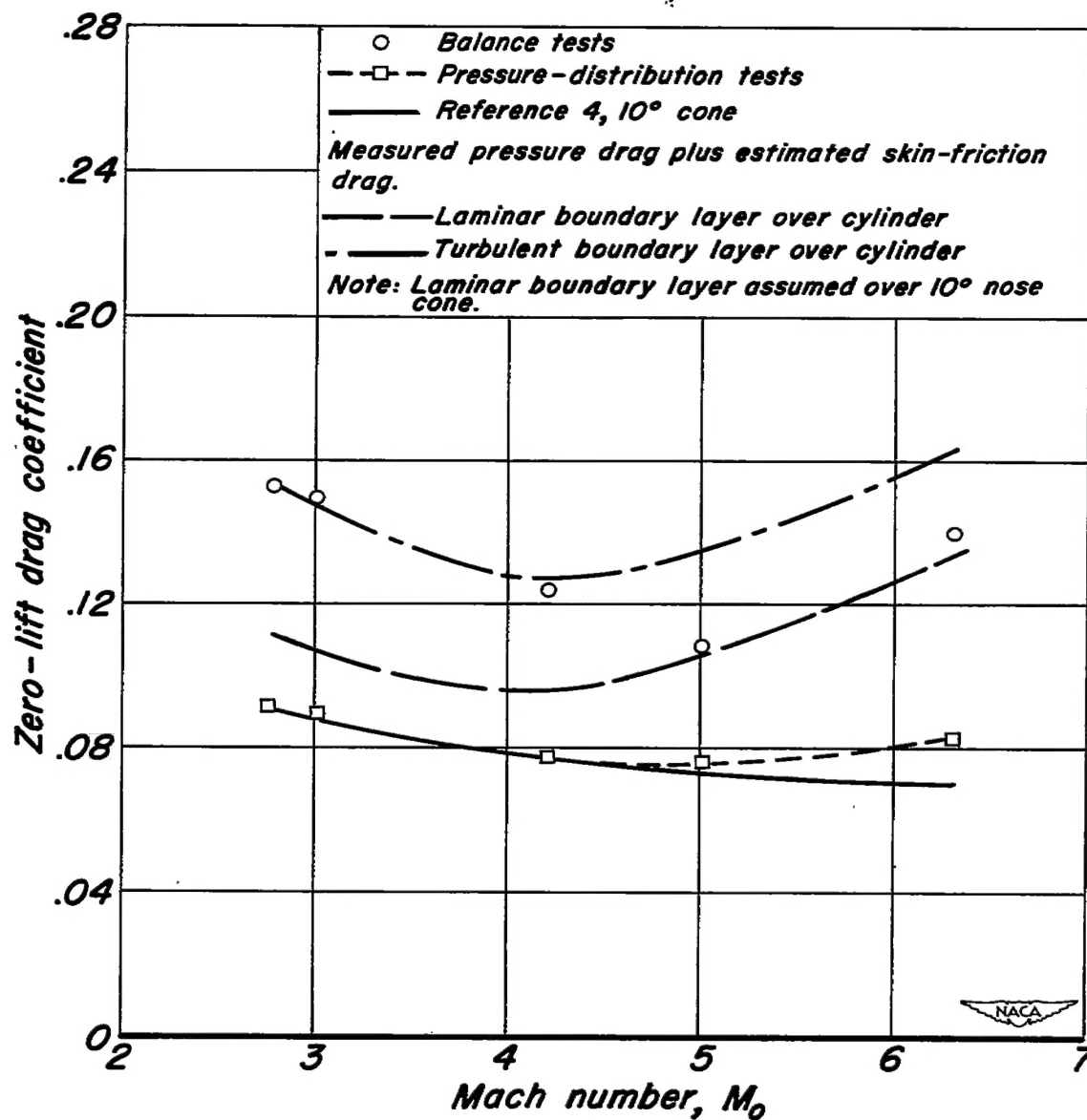


Figure 6.- Variation of zero-lift drag coefficient with Mach number for ballistic missile.



~~CONFIDENTIAL~~



~~CONFIDENTIAL~~